

Dynamical correlations across the spin-state transition in LaCoO_3

L. Craco and E. Müller-Hartmann

Institut für Theoretische Physik, Universität zu Köln, 77 Zùlpicher Straße, 50937 Köln, Germany

(Received 17 October 2006; revised manuscript received 20 March 2007; published 25 January 2008)

The electronic properties of LaCoO_3 across the spin-state transition are studied using the LDA+DMFT method. Combining the local density approximation band structure of the Co $3d$ orbitals in the low-spin state with multiorbital dynamical mean field theory for $U=5$ eV, we investigate the evolution of the single-particle spectra at different spin states. We show that small differences in the orbital occupation can induce a smooth *spin-state crossover* due to large dynamical renormalizations of the energy splitting between the t_{2g} and e_g manifolds. We find large changes in the one-particle spectra that are unique fingerprints of each of the possible spin states. The key signature of the intermediate- and high-spin states is the presence of Hubbard satellites in the t_{2g} spectral density. Further, our results for the paramagnetic metallic phase shows Kondo-like resonance in the t_{2g} sector, indicating the role of multiorbital Kondo screening processes in the high-spin state. These results provide a theoretical basis for physics of room-temperature thermoelectric materials based on cobalt oxides.

DOI: [10.1103/PhysRevB.77.045130](https://doi.org/10.1103/PhysRevB.77.045130)

PACS number(s): 71.28.+d, 71.30.+h

I. INTRODUCTION

LaCoO_3 has been extensively studied due to very interesting properties, most of them in connection with the insulator-metal transition (IMT) induced by changes in temperature^{1,2} or doping concentration.^{3,4} Particularly interesting are the Sr doped samples ($\text{La}_{1-x}\text{Sr}_x\text{CoO}_3$) which become ferromagnetic for $x > 0.2$.⁵ Furthermore, LaCoO_3 exhibits gradual spin-state transitions from nonmagnetic (semiconductorlike) at low temperatures to a paramagnetic insulating state above 90 K and to a metal above 500 K.^{1,2} These effects were proposed to be driven by changes in the spin state of the Co^{3+} ion from the low-spin (LS) state to an intermediate-spin state (IS) and then to a high-spin state (HS). Such a new degree of freedom is favored in cobalt oxides due to a very delicate energy balance between the crystal-field energy and Hund's coupling.

Very subtle effects may cause the spin-state transition in LaCoO_3 ; therefore, it is not surprising that its electronic, magnetic, and transport properties are not completely understood. X-ray diffraction data show a monoclinic distortion in the LS and IS states, with increasing of the Jahn-Teller distortion on thermally activated Co^{3+} ions from LS-to-IS state.⁶ Magnetic susceptibility data⁷ show a maximum at about 100 K and a Curie-Weiss behavior at higher temperatures. These experimental facts along with highly unusual properties in thermal expansion⁷ support a picture where the spin-state transition is driven by *thermal population* of the e_g orbitals accompanied by a structural feedback of an increase in the Co-O bond length.^{8,9}

Hallmarks indicating the importance of multiorbital electron-electron interactions are seen in the optical- and one-particle electron-spectroscopy measurements. With the increase of the temperature or doping concentration, the optical (conductivity) data change over a large energy range.⁹ Photoemission spectrum (PES) and x-ray absorption spectrum (XAS) reveal further proofs of the correlation-driven scenario of the IMT in LaCoO_3 . Low- T data show spectral weight around 1.2 eV binding energy with a large low-spin Co^{3+} contribution.^{1,2,10} At higher temperatures, appreciable

changes are observed in the PES spectra across the spin-state transition, with a characteristic transfer of spectral weight from high to low energies over a scale of almost 4 eV. This implies a drastic rearrangement of the electronic states over a wide energy range (see our results below). Similar effects are also seen in the $1s$ XAS.¹ In these measurements, the low- T spectra develop from a single contribution at about 1 eV into two components for temperatures above 550 K. The origin of this additional structure has been interpreted as a signature of a mixed-spin state, where the Co $3d$ bands are split due to crystal-field effects. In contrast to this interpretation, our results indicate that the lower energy component originates from thermally activated carriers closing the Mott-Hubbard gap in both t_{2g} and e_g orbitals.

Many theoretical efforts have been made to understand the spin-state transition¹¹⁻²¹ in LaCoO_3 (most of them based on band-structure and cluster-model calculations), but the underlying electronic structure across the spin-state transition has not been clarified. In particular, it is not clear how important the role of the multiorbital electron-electron interactions across the spin-state transition is. Is it the tendency to increase the number of electronic degrees of freedom which drives the transition? What is the specific relation between temperature and the spin-state transition? Apart from a consistent description of the experimental facts mentioned above, a successful theoretical picture of the spin-state transition should address these questions systematically. In this work, we discuss a theoretical scenario extending earlier works^{11,12,18-21} in the light of the above requirements.

Band-structure calculations combined with the fixed-spin-moment (FSM) method have been used to determine the energy difference between the spin states.¹⁸ The FSM scheme is based on the assumption that the total energy of the system is minimized under the condition that the total spin moment is fixed at a prescribed value.^{21,22} Magnuson *et al.*,¹⁸ for example, assume in their work that the constrained magnetic moments of the Co^{3+} ion are 0 (LS), 2 (IS), and $4\mu_B$ /f.u. (HS) to investigate the temperature-dependent resonant soft x-ray spectroscopy of LaCoO_3 . *Ab initio* band-structure¹⁸ calculations, including the LDA+ U (Ref. 12) approximation, obtain spin-polarized spectral density in the IS and HS con-

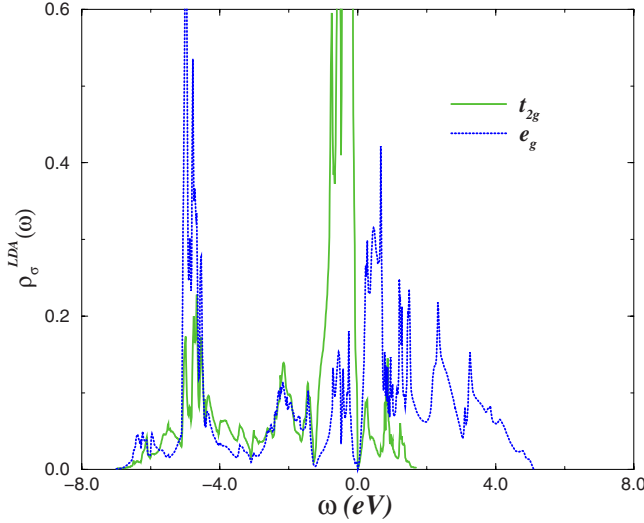


FIG. 1. (Color online) LDA partial density of states for the e_g (dotted) and t_{2g} (solid) orbitals in the LS state taken from Ref. 20.

figurations. This result is problematic in view of the paramagnetic nature of both IS and HS states. Furthermore, the *metallic* solution obtained in Refs. 12 and 18 for the insulating-IS state is also inconsistent with experimental data, clearly indicating the importance of strong dynamical electron-electron interactions in LaCoO₃. With these caveats, in what follows, we analyze the effects of multi-orbital Coulomb interactions across the spin-state transition in LaCoO₃.

To provide new insights into the mechanism which leads to different spin states, we follow the FSM scheme keeping the paramagnetic phase intact. Consistent with FSM ideas, we will assume that a particular spin state is prescribed by fixing the e_g and t_{2g} orbital occupations. We employ this methodology within the LDA+DMFT²³ scheme to analyze the effect of multi-orbital electron-electron interactions on the single-particle spectrum. Good qualitative agreement with inverse-photoemission spectrum (IPES) is obtained within this picture. However, in view of our restriction to the 3d sector, our work should be considered as the first step toward a more detailed description of temperature-,^{1,2} pressure-,²⁴ or light-induced²⁵ spin-state instabilities and mixed-spin-state configurations^{26,27} in cobalt oxides.

II. MODEL AND SOLUTION

We start with the local density approximation (LDA) band structure of LaCoO₃ in the rhombohedral structure corresponding to the LS state.²⁰ The LDA density of states (DOS) computed using experimental crystallographic data shows very interesting one-particle features. First, a sharp peak just below the Fermi level corresponding to the Co⁺³ LS configuration is seen in the t_{2g} spectra in Fig. 1. In addition, the e_g states are known to be strongly hybridized with the O 2p orbitals producing a broader band about 12 eV wide. The structures appearing near the bottom of the valence band in both e_g and t_{2g} spectra are covalent contributions originating from Co–O bonds in the distorted cubic structure. Finally,

from the LDA DOS, one can compute the occupation of each orbital in the LS configuration by integrating it up to the Fermi level: $n_{\sigma}^{t_{2g}}=0.93$ and $n_{\sigma}^{e_g}=0.48$. Note that the relatively large occupancy of the e_g is the signature of a highly covalent ground state.

The one-electron part (LDA band structure) of the multi-orbital Hamiltonian is

$$H_0 = \sum_{\mathbf{k}\alpha\beta\sigma} \epsilon_{\alpha\beta}(\mathbf{k}) c_{\mathbf{k}\alpha\sigma}^{\dagger} c_{\mathbf{k}\beta\sigma} + \sum_{i\alpha\sigma} \epsilon_{i\alpha\sigma} n_{i\alpha\sigma}, \quad (1)$$

where $\alpha, \beta = t_{2g}, e_g$, denoting the fivefold 3d sub-basis, with triply degenerate t_{2g} and doubly degenerate e_g bands. We shall notice that in view of large covalence effects, a correlated *ab initio* description of the full many-body spectrum of LaCoO₃ should in principle incorporate in a single picture all relevant orbitals which come from O 2p and Co 3d bands. However, as far as the spin-state transition is concerned, we will consider only the Co 3d manifold in what follows. Additionally, we will assume that orbital splitting in the t_{2g} and e_g sectors will have minor effect due to the strongly correlated nature of the multi-orbital spectra. To avoid double counting of interactions already treated on the average by LDA, we write

$$H_{LDA}^{(0)} = \sum_{\mathbf{k}\alpha\beta\sigma} \epsilon_{\alpha\beta}(\mathbf{k}) c_{\mathbf{k}\alpha\sigma}^{\dagger} c_{\mathbf{k}\beta\sigma} + \sum_{i\alpha\sigma} \epsilon_{i\alpha\sigma}^0 n_{i\alpha\sigma}, \quad (2)$$

where $\epsilon_{i\alpha\sigma}^0 = \epsilon_{i\alpha\sigma} - U(n_{i\alpha\bar{\sigma}} - \frac{1}{2}) + \frac{1}{2}\sigma J_H(n_{i\alpha\sigma} - 1)$,¹⁶ with $J_H \equiv (U - U_{\alpha\beta})/2$ and $U, U_{\alpha\beta}$ defined in the full many-body model Hamiltonian

$$H = H_{LDA}^{(0)} + U \sum_{i\alpha} n_{i\alpha\uparrow} n_{i\alpha\downarrow} + \sum_{i\alpha\beta\sigma\sigma'} U_{\alpha\beta} n_{i\alpha\sigma} n_{i\beta\sigma'} - J_H \sum_{i\alpha\beta} \mathbf{S}_{i\alpha} \cdot \mathbf{S}_{i\beta}. \quad (3)$$

Cluster-model analysis of spectroscopic data gives $U \approx 5.0$ eV.^{11,17} Given the uncertainty in the precise estimation of U ,^{3,20} we choose $U=5$ eV, $J_H \approx 1.0$ eV, and $U' \equiv U_{\alpha\beta} = 3.0$ eV in the calculations below.

In the 3d sub-basis which diagonalizes the one-particle density matrix, we have $G_{\alpha\beta\sigma\sigma'}(\omega) = \delta_{\alpha\beta} \delta_{\sigma\sigma'} G_{\alpha\sigma}(\omega)$ and $\Sigma_{\alpha\beta\sigma\sigma'}(\omega) = \delta_{\alpha\beta} \delta_{\sigma\sigma'} \Sigma_{\alpha\sigma}(\omega)$. The LDA+DMFT solution for the paramagnetic and paraorbital phase involves replacing the lattice model by a multi-orbital, asymmetric Anderson impurity model and a self-consistency condition requiring the impurity propagator to be equal to the local (k averaged) Green function of the lattice, i.e.,

$$G_{\alpha}(\omega) = \frac{1}{N} \sum_{\mathbf{k}} \frac{1}{\omega + \mu - \sum_{\alpha'} [\omega, \mathcal{A}_{\alpha'}(\omega)] - \epsilon_{\mathbf{k}\alpha}} = \frac{1}{\omega + \mu - \sum_{\alpha'} [\omega, \mathcal{A}_{\alpha'}(\omega)] - \mathcal{A}_{\alpha}(\omega)}, \quad (4)$$

with $\mathcal{A}_{\alpha}(\omega)$ being the dynamical Weiss field for orbital α . Further, since $U_{\alpha\beta}$ scatters electrons between the Co 3d bands, only the total number $n_t = \sum_{\alpha} n_{\alpha} = n_{e_g} + n_{t_{2g}}$ is conserved in a way consistent with Luttinger's theorem. To solve the DMFT impurity problem, we use the iterated perturbation

theory (IPT), generalized to finite temperatures at arbitrary fillings.²⁸ The corresponding local self-energies $\Sigma_a(\omega)$ are computed within the multiorbital IPT (MO-IPT) scheme (see discussion below),²⁹ which account for the first few moments of the spectral functions,^{30,31} guaranteeing the correct low- and high-energy behaviors of the Green's functions, and are solved self-consistently with respect to these constraints.

III. COMMENTS ON IMPURITY SOLVERS

The LDA+DMFT²³ is a suitable tool to describe the interplay between strong multiorbital Coulomb interactions and itinerance (LDA spectra) in real three dimensional compounds. The central difficulty in this scheme is the choice of an appropriate impurity solver to solve the multiorbital, asymmetric Anderson impurity problem. Two ways have been used with varying degrees of success: MO-IPT and quantum Monte Carlo (QMC). The noncrossing approximation³² and exact diagonalization³³ have also been used in this context.

In this work, we use a multiorbital extension of IPT²⁹ to solve the impurity problem of LaCoO₃. This approach is valid if the behavior of the multiorbital impurity problem is analytic in $U(U')$: this is known to hold for the general asymmetric version. The MO-IPT has the advantage of being extendable to all temperatures, and the self-energies can be extracted at modest numerical cost. It is understood that this method is by no means exact, and calculations done for the multiband Hubbard model²³ show quantitative differences with QMC results. However, direct comparison between these two methods is not always possible within the multi-orbital framework—the comparison between these two solvers is feasible when the temperature is so high that QMC will not have sign problems. Recently, we have made a few attempts³⁴ to compare our results with other recent works which use QMC to solve the impurity problem of the DMFT equations. As in the case of the one-band Hubbard model, we found that the position of the lower and the upper Hubbard bands as well as the Mott-Hubbard gap are all in good agreement with the QMC calculations.

Let us recall that extensions of the one-orbital IPT to the multiorbital case were attempted by different groups. In this respect, Fujiwara *et al.*³⁵ did a systematic study on doping-driven insulator-metal transition in doubly degenerated e_g orbitals. Saso³⁶ incorporated ideas developed by Yeyati *et al.*³⁷ to study the periodic Anderson model with N -fold degeneracy. Kotliar *et al.*²³ have also implemented the IPT scheme and, further, used it to account for the effect of electronic correlations in multiband systems. The idea behind MO-IPT is actually not new and it was introduced by Yeyati *et al.*³⁷ who developed it in the context of multilevel quantum dots. This multiorbital version of the *modified* perturbation theory for the single impurity Anderson model was further generalized to the lattice case by Pou *et al.*³¹ Thus, the (MO)-IPT is clearly a well established tool, and it has been applied for a wide variety of correlated electron systems with a nice degree of success.

IV. RESULTS AND DISCUSSION

To proceed, we use the *analogy* between the FSM and the constrained t_{2g} orbital occupation^{12,18} to derive the spin-state

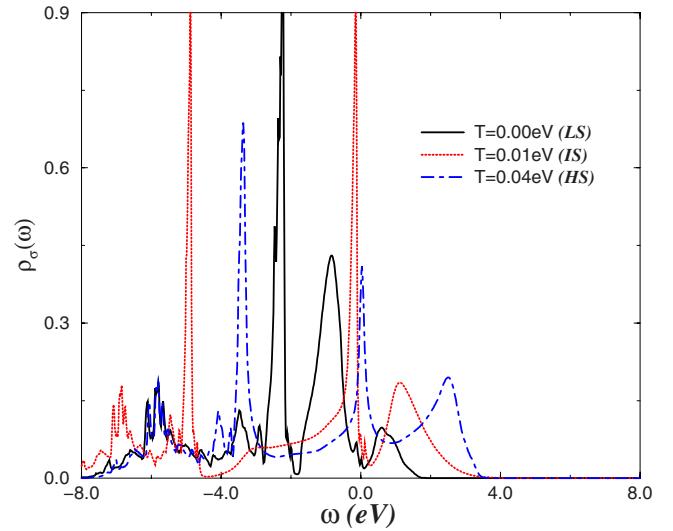


FIG. 2. (Color online) Partial density of states of the t_{2g} orbitals for $U=5.0$ eV in the low-spin (solid), intermediate-spin (dotted), and high-spin (dot dashed) states of LaCoO₃.

transition. Within our LDA+DMFT scheme, we search for the correct values of the fully renormalized atomic levels of all $3d$ orbitals to ensure the most probable t_{2g} orbital occupation of a particular spin-state configuration. To be consistent with our input LDA DOS, we fix the total number of electrons to $n_t \approx 7.5$.²⁰ This value corresponds to the bare (LDA) occupation of each Co atom in the LS phase. Here, we will assume slightly smaller values for the IS and HS t_{2g} orbital occupancies when compared with those obtained by Korotin *et al.*¹² Their constrained t_{2g} orbital occupancies are 0.83 (IS) and 0.675 (HS). Our choice is consistent with the fact that LDA+ U (Ref. 12) calculations gives larger t_{2g} orbital occupation than the LDA ones²⁰ for the LS state.

In our treatment, the t_{2g} electron energies $\epsilon_{t_{2g}}$ are self-consistently adjusted to ensure the expected orbital occupation of a particular spin state. In the course of this procedure, we change the occupation of the t_{2g} orbitals and monitor their fully renormalized spectral functions along with the changes in the single-site occupation of the doubly degenerated e_g bands. More explicitly, we search for the correct values of the fully renormalized atomic energies [driven by changes in the chemical potential μ , see Eq. (4)] for different values of the t_{2g} occupation and fixed total number of electrons n_t . In doing so, we self-consistently adjust both the one-site energy $\epsilon_{t_{2g}}$ and the chemical potential μ . Here, multi-orbital correlations have very important effects. Given a trial value of $\epsilon_{t_{2g}}$ and μ , correlations in the system strongly renormalize the bare energies due to multi-orbital Hartree shifts originating from U , U' , and J_H , leading to large spectral weight transfer upon small changes in the orbital occupation. The Green's functions of the multi-orbital problem for LaCoO₃ [Eq. (3)] are solved self-consistently with MO-IPT until we achieve convergence for the self-energies and the orbital occupations.

In Fig. 2, we show our results for the partial t_{2g} DOS in the low-spin (LS: $t_{2g}^6 e_g^0$), intermediate-spin (IS: $t_{2g}^5 e_g^1$), and high-spin (HS: $t_{2g}^4 e_g^2$) states. As one can see, the LS spectrum

computed assuming the bare LDA value ($n_{\sigma}^{t_{2g}}=0.93$) strongly differs from the LDA results (see Fig. 1 for comparison). First, due to strong multiorbital scattering processes, the narrow t_{2g} band below the Fermi level ($\omega=0$) splits into two subbands at -1.8 eV. The spectral density of the *renormalized* valence band near the Fermi level and the peak at 0.85 eV binding energy are in good agreement with valence band (PES) measurements in the LS state.^{1,10}

The IS spectra calculated at $T=0.01$ eV ≈ 116 K (the temperature where the LS-to-IS state transition is expected to take place^{19,24,26}) and $n_{\sigma}^{t_{2g}}=0.93(1-\frac{1}{6})=0.77$ are accompanied by large spectral weight transfer as compared to the LS case. Interesting are the Hubbard satellites, which are never captured by LDA+ U or GGA+ U calculations. As one can see in Fig. 2, a large fraction of the spectral weight now appears at the satellites at around -3 and 1 eV as well as at the correlation-driven bonding state at energies about -5 eV. While in the LS and IS states we observe a pseudogap feature near the Fermi level (in agreement with what is seen from PES and/or IPES^{1,2}), the HS ($n_{\sigma}^{t_{2g}}=0.93 \times \frac{2}{3}=0.62$) results show clear signatures of multiorbital Kondo physics. In particular, there are a narrow Kondo-like peak³⁸ at the Fermi level and two pronounced Hubbard satellites at high energies. According to our results, the width of the Kondo peak for $T=0.04$ eV is about 0.34 eV, indicating that the multiorbital Kondo screening drives LaCoO₃ into an incoherent metallic state. One should notice that the second component appearing at $T=550$ K in the spectra of Abbate *et al.*¹ has been associated with the t_{2g} bands in the HS configuration. In this respect, the Kondo-like response appearing in the metallic HS state (Fig. 2) is the first theoretical evidence of the low-energy component observed in PES and IPES experiments.¹ Taken together, our results clearly exclude the simple scenario of a rigid gap closing of a band insulator,^{11,12,19} in spite of the nonmagnetic insulating ground state. Furthermore, they underline the importance of multiorbital electron correlations in LaCoO₃.

We also observe large energy-scale changes of the e_g one-particle spectra. Figure 3 shows a clear Mott-Hubbard gap in the LS state solution. Differently from the t_{2g} spectra (see Fig. 2), the e_g charge gap is strongly reduced in the IS state. In addition, apart from a clear broadening of the renormalized spectra, the many-body Kondo features are not clearly seen in the HS state. This is consistent with the fact that both the bandwidth³⁹ and the band filling control the Kondo physics also in multiorbital systems, assuming, as we did in our theory, fixed values of U and U' . Further, the shoulder originating from the Co-O covalent bonding at about -6 eV is also affected by correlations. Here, virtual scattering processes between the e_g and t_{2g} bands along with multiorbital Hartree shifts transfer spectral weight to higher binding energies.

The spin-state transition is accompanied by large changes in the center of gravity δ of the Co $3d$ manifold. Defining $\Delta \equiv \delta_{e_g} - \delta_{t_{2g}}$ as the value of the e_g-t_{2g} energy splitting, within the LDA+DMFT (IPT) scheme, we obtain $\Delta_{LS}=0.95$ eV, a value which is in good agreement with LDA ($\Delta=0.9$ eV). Our results for the IS ($\Delta_{IS}=-0.35$ eV) and the HS ($\Delta_{HS}=-1.64$ eV) indicate that the energy splitting not

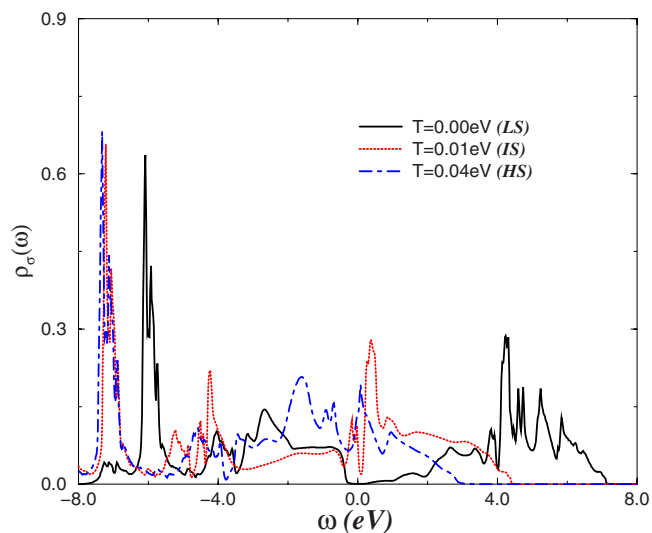


FIG. 3. (Color online) Partial density of states of the e_g orbitals for $U=5.0$ eV in the low-spin (solid), intermediate-spin (dotted), and high-spin (dot dashed) states of LaCoO₃.

just increases by magnitude but changes its sign during the spin-state transition. The change in sign of Δ is an interesting aspect of our theory and it might be the mechanism which stabilizes the HS state at high temperatures. Finally, to highlight the influence of the orbital splittings on the correlated nature of different spin-states, in Fig. 4, we show the total DOS ($\rho_{tot}=\sum_{\alpha\sigma}\rho_{\alpha\sigma}$) obtained at $T\leq 0.01$ eV. As seen in this figure, the one-particle spectra span over large energy scales despite of not too large changes in the corresponding orbital occupations. This dynamical effect is characteristic of correlated multiorbital systems and will have implications when comparing theory with experiment (see below).

The effect of temperature in the HS configuration is shown in Fig. 5. For fixed values of the e_g and t_{2g} orbital occupation, the narrow (low T) Kondo resonance decreases

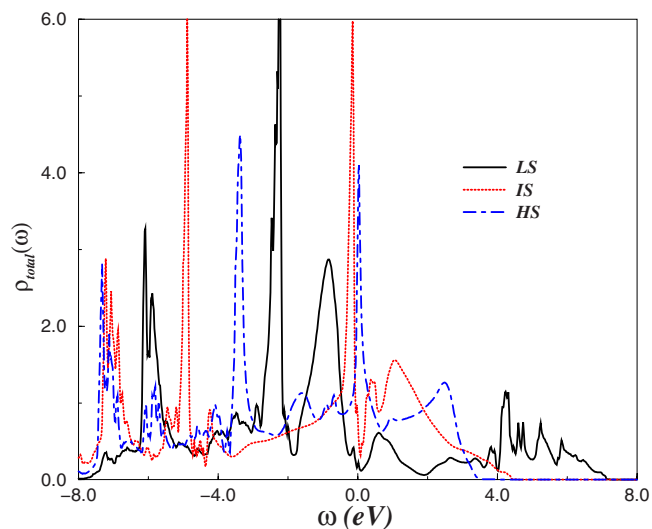


FIG. 4. (Color online) Low- T $3d$ LDA+DMFT total density of states in the low-spin (solid), intermediate-spin (dotted), and high-spin (dot dashed) states of LaCoO₃.

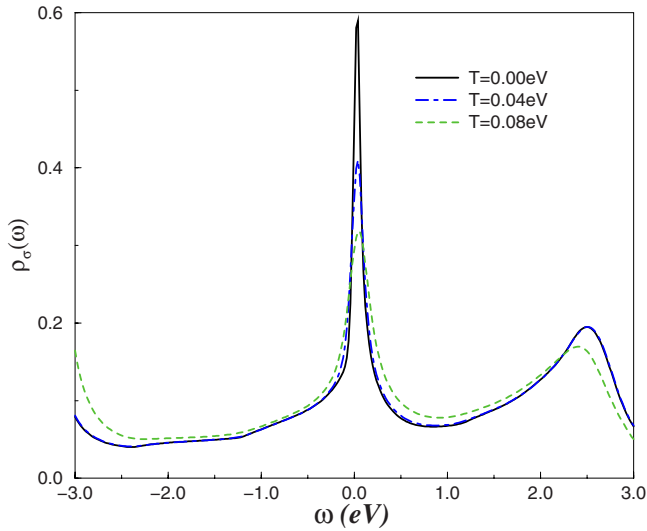


FIG. 5. (Color online) Partial density of states of the t_{2g} orbitals in the high-spin state for $U=5.0$ eV and different temperatures.

as temperature is increased, demonstrating the strength of the multiorbital Kondo effect in the HS state. From the real part of the one-particle self-energy (not shown) at $T=0.005$ eV, we find $\partial \Sigma'_{t_{2g}}(\omega)/\partial \omega|_{\omega=0} = -7.57$, leading to a mass enhancement in the HS state of $m^*/m \approx 8.6$ at very low temperatures. These properties have a natural interpretation in terms of the multiorbital Kondo physics. Let us first recall that coherent Kondo screening has never been the central issue in cobalt oxides despite its strong thermoelectric (power) response.⁴¹ Only recently attention has been given to this effect in connection with Na_xCoO_2 .⁴⁰ In LaCoO_3 , the controversy lies on the two-particle response, where neither optical conductivity nor resistivity shows a clear Fermi liquid response.⁹ (Such type of many-body response has been observed in a host of correlated electron systems, and the coherent state is usually suppressed for temperatures above the Kondo temperature.) However, based on our results (Fig. 5), we conclude that the t_{2g} one-particle spectra in the HS state is characteristic of a Kondo system. The multiorbital Kondo resonance shown in this figure is driven by strong scattering processes involving the very narrow part of the t_{2g} spectra near half-filling. (This electron configuration follows from the HS state.) Additionally, asymmetric screening processes involving the e_g and t_{2g} manifolds, which are responsible for the broad bands seen in Figs. 2 and 3, will be operative to some extent. The emergence of the multiorbital Kondo effect in the HS state provides a natural interpretation for the high unusual thermoelectric response for LaCoO_3 in the low Ca(Sr) doping regime.⁴¹ According to our results, such an unusual response is induced by the strong enhancement of the electron effective mass due to large Kondo screening processes in the t_{2g} orbitals.

V. COMPARISON WITH EXPERIMENT

We now compare our LDA+DMFT (MO-IPT) calculations to published experimental results,¹ with attention to

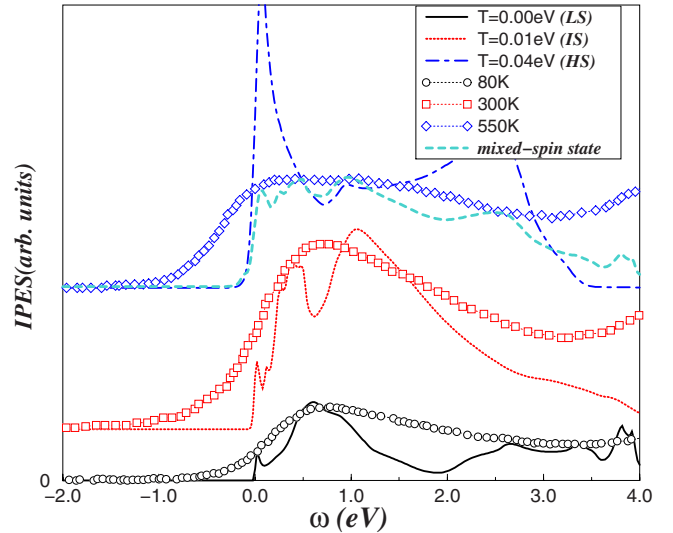


FIG. 6. (Color online) Comparison of theoretical LDA+DMFT (IPT) calculations for the unoccupied part of the total one-electron spectral function at different spin-state phases of LaCoO_3 to the experimental results taken from Ref. 1 for XAS. The intensity of the experimental curves is normalized to coincide with theory.

IPES. Comparison with PES spectra is not possible within our approach. As explained below, this requires us to compute the full one-particle local spectral function (total DOS) including the oxygen bands, which is out of the scope of this work.

In Fig. 6, our results for $U=5$ eV are compared with the experimental work of Ref. 1. The intensity of the XAS is normalized to coincide with theory. Good *qualitative* agreement is observed in the LS state. Differently from the interpretation given in Ref. 1, the main peak at 0.6 eV (529.2 eV in experiment) is mainly due to the unoccupied t_{2g} bands since the e_g band is located at higher energies (see Fig. 3 for details). Therefore, within our scheme, we assign the single contribution above the Fermi level in the LS configuration as the t_{2g} upper Hubbard band. In the IS state, all $3d$ bands contributed to the low-energy onset. We now identify two peaks, where in experiment only one is visible. The lower peak at 0.4 eV is mainly e_g -like, while the second one at 1.06 eV is a combination of unoccupied e_g and t_{2g} subbands. The t_{2g} contribution is higher in energy: this is the fingerprint of strong multiorbital electron interactions in this sector, which is enhanced in going from IS to HS state. In the HS state, the upper Hubbard bands are found at 2.5 eV above the Fermi energy. As expected within the DMFT framework, the peak just above the Fermi energy has its origin in the coherent Kondo scattering process, while that at higher energies is the t_{2g} Hubbard satellite.

Clearly, our result for the homogeneous HS state (dot-dashed line) overestimates both the intensity and the energy splitting of the HS peaks. In XAS, the splitting is 2 eV smaller than the one predicted here.¹ However, a better fit of the high- T spectra is obtained if one assumes the mixed-spin-state scenario.^{1,27} Within this scenario, we find qualitative agreement with experiment by averaging the total spectral function ($\rho_{\text{tot}} = \rho_{t_{2g}} + \rho_{e_g}$) of different spin states using the fol-

lowing ratios: LS:45%, IS:30%, and HS:25%. For the HS population, we employ a value similar to that predicted in Ref. 27. With our choice for the IS and LS populations, good agreement over almost the whole energy scale from $0 \leq \omega \leq 3$ eV is observed in Fig. 6. The low-energy component of the one-particle spectra in the HS state has a large t_{2g} contribution, in agreement with the analysis of Ref. 1. Based on our results (Figs. 2 and 3), the peak 1 eV above the Fermi energy (529.2 eV in XAS) is related to the unoccupied mixed-spin state, where all spin configurations contribute in this phase. The intensity of the experimental XAS data is sensitive to the partial IS contribution. Our result differs from the interpretation given in Refs. 1 and 27, where the HS state is seen as a mixed-spin state composed of LS and HS configurations. Here, we show that the IS contribution is relevant for a concrete description of the XAS spectra in the HS state. More experimental and theoretical work is needed to resolve whether this can also explain the T dependence of the full one-particle spectral function of LaCoO_3 .

Consideration of the spectrum for energies below the Fermi level (PES) and for $\omega > 3.0$ eV (IPES) is limited by our restriction to the $3d$ sector. Since in our LDA+DMFT calculations we have ignored contributions from the oxygen bands, we cannot account for spectral weight changes at energies below the Fermi level. We also see that some spectral weight is lost in the IPES spectra, possibly due to the lack of La bands.^{11,15} Thus, our work should be regarded as an attempt toward a more concrete LDA+DMFT description of the spin-state transition in LaCoO_3 and related compounds. Finally, we shall notice that our work shares some similarities with the theory of Ren *et al.* for NiO , a charge transfer insulator with strong $p-d$ hybridizations.⁴² Also interesting in this context is the work by Kunes *et al.* for the same compound.⁴³ The outcome of these two LDA+DMFT studies is in very good agreement with the upper part of the single-particle spectrum. The lower part seems to depend on the tiny details of the one-body Hamiltonian and on how one-electron degrees of freedom are implemented within the LDA+DMFT scheme. To shed more light on the dynamical responses of LaCoO_3 across the spin-state transition, future LDA+DMFT studies should follow the strategy of Ref. 43 to incorporate the oxygen p bands in the multiorbital problem.

VI. CONCLUDING REMARKS

In this work, we underline the importance of electron correlations across the spin-state transition in LaCoO_3 using the LDA+DMFT scheme. The spin-state transition is seen as a smooth spin-state *crossover* accompanied by changes in orbital occupation in the e_g and t_{2g} sectors, strongly increasing the energy splitting between the e_g and t_{2g} shells of the cobalt ions. Our results support a metallic high-spin state and two distinct insulating (low and intermediate spin) phases, consistent with a host of experiments.^{1,2,9,24} We obtain good qualitative agreement with published inverse-photoemission

data,¹ suggesting that similar ideas can be applied to study thermal and optical responses as well as doping effects. The fact that in the LS and IS states the Fermi level is lying in a pseudogap valley indicates that LaCoO_3 is close to a Mott-Hubbard insulator-metal transition, which can be induced by changes in the $t_{2g}-e_g$ orbital occupation.

We have shown that the depopulation of the t_{2g} orbitals strongly enhances the low-energy electronic degrees of freedom of the cobalt ions. In light of this result, one can argue that the gain in entropy induced by spins and charge fluctuations in the HS state spontaneously drives the spin-state transition. The entropy gain across the spin-state transition is understood as follows. First, the depopulation of the t_{2g} bands favors electron transfer between different orbitals (both e_g and t_{2g}), increasing local spin and charge fluctuations in the Co^{3+} ions.⁴⁴ Second, the t_{2g} -electron hopping allows for virtual changes the ionic configuration from Co^{3+} to Co^{4+} as the electrons hop to the neighboring cobalt sites via oxygen. This dynamical electron motion between sites and orbitals changes the total occupation of the local ions increasing the charge and spin entropies,⁴⁵ explaining the relation between temperature and the spin-state transition. Taken together, it seems that the higher paramagnetic entropy of the HS state is very important in driving the spin-state transition in cobalt oxides^{44,45} and other transition metal compounds.⁴⁶

To conclude, our results for the homogeneous HS metallic state shows a Kondo-like response in the t_{2g} sector, which so far has not been experimentally detected. The lack of orbital Kondo fingerprints in the HS quasiparticle spectra can be explained in terms of an inhomogeneous distribution of various spin states. In this peculiar regime, a particular spin state became a mixture of two or, as we have shown, three different spin configurations. This understanding is consistent with the recent experimental study by Haverkort *et al.*,²⁷ which concludes that an inhomogeneous mixed-spin-state system (made of LS and HS components) is formed at finite temperatures. Notice, however, that a nonhomogeneous distribution of various spin configurations would be an intrinsic source of disorder in the system, strongly determining both spin and charge responses at intermediate and high temperatures. To clarify this and the above issues, more experimental and theoretical work is needed. In fact, it would be interesting to search for new routes to a HS state keeping the multiorbital Kondo physics intact. This might be a thriving perspective for the next generation of thermoelectric cooling materials, due to intrinsic low electric resistivity and high (charge and/or spin) entropy of multiorbital Kondo systems.

ACKNOWLEDGMENTS

L.C. acknowledges D. I. Khomskii, M. S. Laad, H. Wu, and T. Lorenz for useful discussions and remarks. This work is done under the auspices of the Sonderforschungsbereich 608 of the Deutsche Forschungsgemeinschaft.

- ¹M. Abbate, J. C. Fuggle, A. Fujimori, L. H. Tjeng, C. T. Chen, R. Potze, G. A. Sawatzky, H. Eisaki, and S. Uchida, *Phys. Rev. B* **47**, 16124 (1993).
- ²T. Saitoh, T. Mizokawa, A. Fujimori, M. Abbate, Y. Takeda, and M. Takano, *Phys. Rev. B* **55**, 4257 (1997).
- ³A. Chainani, M. Mathew, and D. D. Sarma, *Phys. Rev. B* **46**, 9976 (1992).
- ⁴T. Saitoh, T. Mizokawa, A. Fujimori, M. Abbate, Y. Takeda, and M. Takano, *Phys. Rev. B* **56**, 1290 (1997); A. R. Moodenbaugh, B. Nielsen, S. Sambasivan, D. A. Fischer, T. Friessnegg, S. Aggarwal, R. Ramesh, and R. L. Pfeffer, *ibid.* **61**, 5666 (2000); M. Kriener, C. Zobel, A. Reichl, J. Baier, M. Cwik, K. Berggold, H. Kierspel, O. Zabara, A. Freimuth, and T. Lorenz, *ibid.* **69**, 094417 (2004).
- ⁵J. B. Goodenough, in *Progress in Solid State Chemistry*, edited by H. Reiss (Pergamon, London, 1971), Vol. 5, p. 145; R. Caciuffo, D. Rinaldi, G. Barucca, J. Mira, J. Rivas, M. A. Señarís-Rodríguez, P. G. Radaelli, D. Fiorani, and J. B. Goodenough, *Phys. Rev. B* **59**, 1068 (1999); R. P. Haggerty and R. Seshadri, *J. Phys.: Condens. Matter* **16**, 6477 (2004).
- ⁶G. Maris, Y. Ren, V. Volotchaev, C. Zobel, T. Lorenz, and T. T. M. Palstra, *Phys. Rev. B* **67**, 224423 (2003).
- ⁷C. Zobel, M. Kriener, D. Bruns, J. Baier, M. Grüninger, T. Lorenz, P. Reutler, and A. Revcolevschi, *Phys. Rev. B* **66**, 020402(R) (2002).
- ⁸P. G. Radaelli and S.-W. Cheong, *Phys. Rev. B* **66**, 094408 (2002); T. Vogt, J. A. Hriljac, N. C. Hyatt, and P. Woodward, *ibid.* **67**, 140401(R) (2003).
- ⁹Y. Tokura, Y. Okimoto, S. Yamaguchi, H. Taniguchi, T. Kimura, and H. Takagi, *Phys. Rev. B* **58**, R1699 (1998).
- ¹⁰R. P. Vasquez, *Phys. Rev. B* **54**, 14938 (1996).
- ¹¹M. Abbate, R. Potze, G. A. Sawatzky, and A. Fujimori, *Phys. Rev. B* **49**, 7210 (1994).
- ¹²M. A. Korotin, S. Yu. Ezhov, I. V. Solovyev, V. I. Anisimov, D. I. Khomskii, and G. A. Sawatzky, *Phys. Rev. B* **54**, 5309 (1996).
- ¹³M. Takahashi and J.-i. Igarashi, *Phys. Rev. B* **55**, 13557 (1997).
- ¹⁴M. Zhuang, W. Zhang, C. Hu, and N. Ming, *Phys. Rev. B* **57**, 10710 (1998); H. Takahashi, F. Munakata, and M. Yamanaka, *ibid.* **57**, 15211 (1998).
- ¹⁵P. Ravindran, P. A. Korzhavyi, H. Fjellvag, and A. Kjekshus, *Phys. Rev. B* **60**, 16423 (1999).
- ¹⁶M. Zhuang, W. Zhang, and N. Ming, *Phys. Rev. B* **57**, 10705 (1998).
- ¹⁷H. Takahashi, F. Munakata, and M. Yamanaka, *Phys. Rev. B* **53**, 3731 (1996); **57**, 15211 (1999).
- ¹⁸M. Magnuson, S. M. Butorin, C. Sathe, J. Nordgren, and P. Ravindran, *Europhys. Lett.* **68**, 289 (2004).
- ¹⁹G. Thornton, I. W. Owen, and G. P. Diakun, *J. Phys.: Condens. Matter* **3**, 417 (1991).
- ²⁰I. A. Nekrasov, S. V. Streltsov, M. A. Korotin, and V. I. Anisimov, *Phys. Rev. B* **68**, 235113 (2003).
- ²¹K. Knížek, P. Novák, and Z. Jirák, *Phys. Rev. B* **71**, 054420 (2005).
- ²²For more details, see J. Häglund, *Phys. Rev. B* **47**, 566 (1993) and the references therein.
- ²³G. Kotliar, S. Y. Savrasov, K. Haule, V. S. Oudovenko, O. Parcollet, and C. A. Marianetti, *Rev. Mod. Phys.* **78**, 865 (2006).
- ²⁴R. Lengsdorf, M. Ait-Tahar, S. S. Saxena, M. Ellerby, D. I. Khomskii, H. Micklitz, T. Lorenz, and M. M. Abd-Elmeguid, *Phys. Rev. B* **69**, 140403(R) (2004).
- ²⁵K. Boukheddaden, I. Shteto, B. Horomano, and F. Varret, *Phys. Rev. B* **62**, 14806 (2000).
- ²⁶K. Asai, A. Yoneda, O. Yokokura, J. M. Tranquada, G. Shirane, and K. Kohn, *J. Phys. Soc. Jpn.* **66**, 967 (1997).
- ²⁷M. W. Haverkort, Z. Hu, J. C. Cezar, T. Burnus, H. Hartmann, M. Reuther, C. Zobel, T. Lorenz, A. Tanaka, N. B. Brookes, H. H. Hsieh, H.-J. Lin, C. T. Chen, and L. H. Tjeng, *Phys. Rev. Lett.* **97**, 176405 (2006).
- ²⁸M. S. Laad, L. Craco, and E. Müller-Hartmann, *Phys. Rev. B* **64**, 214421 (2001); see also L. Craco, *J. Phys.: Condens. Matter* **11**, 8689 (1999).
- ²⁹L. Craco, M. S. Laad, and E. Müller-Hartmann, *Phys. Rev. Lett.* **90**, 237203 (2003); M. S. Laad, L. Craco, and E. Müller-Hartmann, *ibid.* **91**, 156402 (2003).
- ³⁰Y. Takehashi and P. Fulde, *Phys. Rev. B* **69**, 045101 (2004).
- ³¹P. Pou, R. Pérez, F. Flores, A. Levy Yeyati, A. Martín-Rodero, J. M. Blanco, F. J. García-Vidal, and J. Ortega, *Phys. Rev. B* **62**, 4309 (2000).
- ³²M. B. Zöfl, Th. Pruschke, J. Keller, A. I. Poteryaev, I. A. Nekrasov, and V. I. Anisimov, *Phys. Rev. B* **61**, 12810 (2000); K. Held, I. A. Nekrasov, N. Blümer, V. I. Anisimov, and D. Vollhardt, *Int. J. Mod. Phys. B* **15**, 2611 (2001).
- ³³C. A. Perroni, H. Ishida, and A. Liebsch, *Phys. Rev. B* **75**, 045125 (2007).
- ³⁴See, for example, M. S. Laad, L. Craco, and E. Müller-Hartmann, *Phys. Rev. B* **73**, 045109 (2006); **73**, 195120 (2006); L. Craco, M. S. Laad, and E. Müller-Hartmann, *J. Phys.: Condens. Matter* **18**, 10943 (2006).
- ³⁵T. Fujiwara, S. Yamamoto, and Y. Ishii, *J. Phys. Soc. Jpn.* **72**, 777 (2003).
- ³⁶T. Saso, *J. Phys.: Condens. Matter* **13**, L141 (2001).
- ³⁷A. L. Yeyati, F. Flores, and A. Martín-Rodero, *Phys. Rev. Lett.* **83**, 600 (1999).
- ³⁸For a detailed discussion on the origin and nature of the Kondo (quasiparticle) peak in multiorbital systems, see, for example, S.-K. Mo, J. D. Denlinger, H.-D. Kim, J.-H. Park, J. W. Allen, A. Sekiyama, A. Yamasaki, K. Kadono, S. Suga, Y. Saitoh, T. Muro, P. Metcalf, G. Keller, K. Held, V. Eyert, V. I. Anisimov, and D. Vollhardt, *Phys. Rev. Lett.* **90**, 186403 (2003); A. K. McMahan, *Phys. Rev. B* **72**, 115125 (2005).
- ³⁹A. Liebsch, *Phys. Rev. Lett.* **91**, 226401 (2003); A. Koga, N. Kawakami, T. M. Rice, and M. Sigrist, *ibid.* **92**, 216402 (2004).
- ⁴⁰K. Miyoshi, E. Morikuni, K. Fujiwara, J. Takeuchi, and T. Hamasaki, *Phys. Rev. B* **69**, 132412 (2004).
- ⁴¹J. Androulakis, P. Migiakis, and J. Giapintzakis, *Appl. Phys. Lett.* **84**, 1099 (2004); H. Masuda, T. Fujita, T. Miyashita, M. Soda, Y. Yasui, Y. Kobayashi, and M. Sato, *J. Phys. Soc. Jpn.* **72**, 873 (2003).
- ⁴²X. Ren, I. Leonov, G. Keller, M. Kollar, I. Nekrasov, and D. Vollhardt, *Phys. Rev. B* **74**, 195114 (2006).
- ⁴³J. Kunes, V. I. Anisimov, A. V. Lukoyanov, and D. Vollhardt, *Phys. Rev. B* **75**, 165115 (2007).
- ⁴⁴I. A. Zaliznyak, J. M. Tranquada, R. Erwin, and Y. Moritomo, *Phys. Rev. B* **64**, 195117 (2001).
- ⁴⁵W. Koshibae, K. Tsutsui, and S. Maekawa, *Phys. Rev. B* **62**, 6869 (2000).
- ⁴⁶For more details, see K. Kaji, M. Sorai, A. J. Conti, and D. N. Hendrickson, *J. Phys. Chem. Solids* **54**, 1621 (1993), and references therein.